ELSEVIER

Thermochimica Acta 392–393 (2002) 339–355

thermochimica acta

www.elsevier.com/locate/tca

Surface finish of injection molded materials by micro-thermal analysis

M. Provatas, S.A. Edwards, N. Roy Choudhury*

Polymer Science Sector, Ian Wark Research Institute, University of South Australia, Mawson Lakes, SA 5095, Australia

Abstract

In typical injection molding processes, surface defects are often encountered, yielding products of inferior part quality. In an effort to identify and eliminate any unwanted finish, surface defects have been created consistently by injection molding and examined via the use of a new technique known as micro-thermal analysis (μTA^{TM}). μTA^{TM} is an analytical form of microscopy that combines atomic force microscopy (AFM) and differential thermal analysis (DTA). The experiment was performed on polycarbonate/acrylonitrile-styrene-acrylate (PC/ASA) injection molded parts, using thermal probes. Surface defects, such as variations in gloss level, were produced on injection molded plaques by changing molding parameters including material temperature and packing pressure. μTA^{TM} results reveal that rubber particle aggregation is one of the reasons for lowering the parts surface finish, also that scans performed at elevated temperatures, show that there were no changes in the polymer's multiphase morphology. Additionally, depth profiling by μTA^{TM} established that PC and ASA are rich at the outermost surface of regions that possess a dull finish, whilst PC is the dominant material in regions of high gloss.

Keywords: Micro-thermal analysis; Polycarbonate; Acrylonitrile styrene acrylate; Injection molding and Surface finish

1. Introduction

Injection molding is the process in which a molten plastic is forced into a cold mold, allowed to cool and solidify to form a specific product [1]. Since polymers are poor thermal conductors, there is a large temperature gradient present when the gate freezes (the gate is the inlet where molten polymer flows through). The interior material continues to cool and shrink but is opposed by the material that has already frozen. This produces thermoelastic stresses in the interior of the plastic resulting in part failure. Additional flow stresses such as shear/extensional stress, generated in the melt during mold filling and partly frozen in as residual stresses, are almost always present in the injection molded article and can pose significant influences over the bulk/surface properties of the moldings.

These stress and thermal shrinkage phenomena often cause product distortion resulting in marred visual appearances. Such defects include discolouration, visible flow patterns, weld lines, pearlescence (gloss variation), sink marks and surface rippling. Other minor defects include scuffing, pitting and cavitation due to material decomposition. Defects that occur on the outer surface of the molded part pose a problem since they lower the surface quality of the finished product. The detection of failed parts due to distortion normally comes quite late in the development cycle and is therefore expensive to solve.

* Corresponding author. Tel.: +61-8-8302-3719; fax: +61-8-8302-3755.
E-mail address: namita.choudhury@unisa.edu.au (N. Roy Choudhury).

0040-6031/02/$ – see front matter
PII: S0040-6031(02)00120-X

However, in any complex manufacturing process, the key to minimising such problems is to completely understand the process, materials and equipment involved.

Previous studies [2] on the effect of injection molding parameters on the properties of molded parts have demonstrated that there are five main controllable factors. These include injection time, material temperature, mold temperature, pack pressure and cavity pressure, all of which play significant roles during the injection cycle to varying degrees. High mold temperatures are known to improve surface appearance significantly. Molten plastic, at elevated temperatures, has a lower viscosity and thus a better flow behaviour, thereby, reducing shear stress. By raising injection time, shear stress also increases, resulting in flow instabilities and therefore a poor surface finish.

Over the past several years there has been considerable amount of work investigating the effects of the packing pressure phase and this has yielded data that recognises this parameter as the single most dominant cause of varying properties in injection molded parts [3,4]. The higher the packing pressure, the higher the yield modulus and ultimate tensile strength of the polymer. This is due to more efficient packing of the material. Additionally, higher molecular orientation is often the result of an increase in pack pressure.

The majority of aesthetic surface defect analysis has predominantly yielded causes such as wall slip and flow instabilities mechanisms [5]. Molecular structure can also play a key role in surface finish. Parts with high values of melt elasticity (recoverable shear strain) are of greater quality when compared with others. The Rouse molecular theory predicts that the melt elasticity should be proportional to the breadth of the molecular weight distribution [6]. Futhermore, improved surface appearance was noted when rubber levels were decreased [5]. However, a smaller gel content will effect the impact strength of the material. Therefore, a balance in the size and content of rubber particles is required to achieve good surface finish and high impact strength.

In the past, defect characterisation has been predominantly accomplished through various microscopical [7], flow visualisation [8] and theoretical methods [5]. However, use of novel surface techniques such as micro-thermal analysis (μTA^{TM}), which can characterise and visualise simultaneously, is an exciting new challenge in the field of polymer chemistry [9].

The μTA^{TM} combines aspects of thermal analysis and atomic force microscopy (AFM) to create a new system for analysing material surfaces. This technology has replaced the conventional AFM tip with a 5 μm diameter, silver-coated platinum filament known as a Wollaston wire [10]. This wire has a synergistic effect, acting as both a heat resistor and temperature sensor and thereby enabling visualisation of a surface (resolution 2–3 μm), by not only topographical means but also via thermal properties. This technique closely examines the surface and near-surface layers of substrates, correlating physical properties and topography with observed phases and boundary layers [11]. Furthermore, it is possible to apply a heating signal to the solid substrate and thus perform localised thermal analysis (LTA) in highly focused areas of interest on the sample [12].

To date, most research conducted with the μTA^{TM}, has been in the realm of pharmaceutical chemistry [10]. Components within a model tablet formulation have been well differentiated using thermal conductivity and LTA methods. Experimental trials have suggested that this method may have significant future in the development of drug dosage forms.

In the field of polymers, μTA^{TM} remains a relatively new technique. Studies to date have included investigations on cross-sectioned packaging film, which contains a gas barrier layer flanked by a 'tie' layer bonding it to the bulk of the film [13]. LTA measurements reveal the barrier layer as comprising poly-(ethylene-co-vinyl alcohol), while the bulk film is high density polyethylene and the tie layer is a low/medium density polyethylene. To date, such information was only possible by a combination of analytical techniques, not via a single technique, making μTA^{TM} a rigorous and handy tool capable of delivering a wealth of information.

The present scope of this work is involved with injection molded thermoplastic blends. No μTA^{TM} studies investigating the morphology of injection molded thermoplastic blends have been published to our knowledge. It is the focus of this present study to use the understanding gained from previous polymeric and pharmaceutical research and to apply it to understanding the cause of defect formation involved in modern injection and injection compression molding,

as a wide variety of surface defects are generally produced by these manufacturing processes.

Surface defects on injection molded thermoplastic components were engineered on polycarbonate/acrylonitrile-styrene-acrylate (PC/ASA) samples by varying such parameters as pack pressure, material temperature and injection speed. Samples at various material temperatures and pack pressures were examined via different thermal techniques, μTA™ as well as dynamic mechanical analyser (DMA). DMA was used to evaluate the storage modulus and glass transition temperatures of the samples. Combining such thermal techniques allows for the investigation of surface defects or morphological differences at key locations on each sample.

2. Experimental

2.1. Materials

Geloy XP4025 PC/ASA, containing a small quantity of polymethylmethacrylate (PMMA), was supplied by GE plastics. Raw pellet material was injection molded into plaques (285 mm × 75 mm × 3 mm) using a Ludgwig 'Engel' model ES 700/150, injection molder (Maschinefabrik Schwertberg, Austria) coupled with a MS plaque tool. Table 1 lists the injection molding processing conditions that were used to produce defected plaques. A total of 15 plaques per condition were manufactured using these settings. An initial purge period was used to dispose of any material remaining from previous runs.

2.2. Techniques

2.2.1. Micro-thermal analysis (μTA™)

μTA™ measurements were performed using the μTA 2990 micro-thermal analyser (TA Instruments) [14–16] with a thermal probe. As the probe scans across the sample surface three images can be obtained: (1) surface topography; (2) thermal conductivity (dc signal); and (3) thermal diffusivity (ac signal).

A performance check was performed on a semiconductor silicon grid, which consists of raised SiO_2 squares with a 3 μm pitch, to determine whether the system was fully operational. The probe was temperature calibrated using polycarbonate and polyethylene of known glass transition temperatures (T_g).

Surface defected PC/ASA plaque samples were sectioned and microtomed (40 μm thickness) to investigate morphology. Scans were performed in AC mode at room temperature, 55 and 80 °C with a modulation frequency of 2 kHz and a modulation amplitude of ±5 °C. Both microtomed and plaque samples were characterised at different locations using LTA, at a heating rate of 10 °C/s in DC mode. To investigate the sub-surface morphology, depth profiling was performed by varying the modulation frequency. Depth profile images of thermal conductivity and thermal diffusivity were acquired at 2 and 64 kHz, respectively, with a modulating amplitude of ±5 °C. All images were scanned in a controlled environmental clean room laboratory, at a scan rate of 100 μm/s, image size 100 μm × 100 μm and resolution 300. All T_g values were determined from the onset of the sensor signal.

2.2.2. Dynamic mechanical analyser (DMA)

DMA Model 2980 (TA Instruments) was used to identify the effect of processing conditions on the T_g and storage modulus values of the PC/ASA plaques. A dual cantilever clamp in the temperature range of −100 to 160 °C at frequencies of 0.1, 1 and 10 Hz, strain amplitude of 0.8 and at a heating rate of 2 °C/min was applied. In this work, T_g was determined from the peak maximum of the loss modulus curves and compared with those determined from μTA™.

Table 1
Injection molding parameters for engineered surface defected plaques, under an ideal injection time

Plaque	Condition	Injection time (s)	Pack time (s)	Material temperature (°C)	Pack pressure (bar)
1	Ideal	2.61	10	260	55
2	Ideal, pack pressure high	2.62	10	260	100
3	Ideal, material temperature high	2.60	10	275	55

3. Results and discussion

3.1. Surface defects

All plaques, even those molded at ideal conditions, displayed a variety of surface defects. Plaque 1 produced the best overall surface finish but was flawed around the edges with a variation in gloss that appeared as a dull line. A sink mark was also evident in the centre of the part and was due to the position of the ejector pins on the other side of the mold. Plaque 2, made at ideal conditions but at a higher pack pressure, showed a similar surface finish as the ideal part. However, surface marks were noted at a position opposite to the location of the gate. The most heavily defected part was Plaque 3, which showed the consistent characteristics of the other two plus stress marks near the gate. The additional temperature in the screw is the likely cause of this finish, with polymer degradation at a more advanced state [17].

3.2. Micro-thermal analysis: morphological study

The bulk/core morphology of injection molded samples was investigated using microtomed samples. The microtomed sections of plaques 1, 2 and 3 have been investigated in both defected (dull, low gloss) and normal (glossy) areas at room temperature, 55 and at 80 °C.

3.2.1. Morphology of normal area (glossy) of the sample

The thermal conductivity and topography (scanned at 55 °C and 2 kHz) images of the normal (glossy) area of the microtomed, injection molded PC/ASA (sample 1), are displayed in Fig. 1a and b. From Fig. 1a, it is evident that the thermal conductivity scan of sample 1 consists of light and dark regions of varying thermal properties. The topography image (Fig. 1b) has also been investigated to find whether there are any topographic artefacts present in the thermal conductivity and thermal diffusivity images. For increased resolution, scans were carried out at 80 °C and show clear domains without altering the multiphase morphology of the polymer (Fig. 2). The morphology of the blend is well visualised and is represented by densely packed, varying sizes of discrete oval and circular-shaped rubber zones of lower conductivity, embedded in a continuous matrix of higher conductivity. There exists a relatively even distribution of rubber zones throughout the matrix, with distinct boundaries visible and little evidence of agglomeration present, a result also observed for the unprocessed material. This is consistent with the structural model of a typical rubber-modified thermoplastic, which consists of both bound and unbound rubber particles within a matrix [18]. Interestingly, at the interface between the rubber phase and the matrix, the conductivity is higher compared to that of the rubber particle itself. These are regions where interphases co-exist and show intermediate thermal conductivity and diffusivity. In such confined regions, mobility of the phase is greatly reduced and restricted. Therefore, glass transition temperatures are likely to be affected in these regions.

Sample 2, produced at a higher packing pressure (100 bar), also shows the presence of three phases. These phases are a result of high packing pressure, a densely packed matrix and a distinct order in packing of the rubber particles. The normal area showed fewer low conductivity particles than sample 1. Sample 3, with a low pack pressure (55 bar) but high material temperature (275 °C), shows a similar alignment of particles.

Diffusivity images for all samples show similar particle orientation as for the conductivity images, being directly related to each other through parameters such as density and heat capacity. These images clearly identify the immiscible, multiphase nature of the material.

3.2.2. Morphology of surface defected (low gloss) sample

Although, it appears somewhat similar to that seen in the unprocessed material (particle size) and in the glossy area, there are however, obvious differences in the conductivity image of sample 1 (dull area). Oval and circular-shaped particles are still visible and multi-phases are evident. Rubber particles (lower conductivity region) are smaller and seen as aggregates, whereas at the higher conductivity regions, single-phase behaviour is predominant. Also, it is clear that particle size is very different from the unprocessed material (10–12 μm, ∼7.7 μm).

Increasing the pack pressure, leads to agglomeration/deformation of the rubber particles in the dull area, as seen in sample 2. It is expected that higher

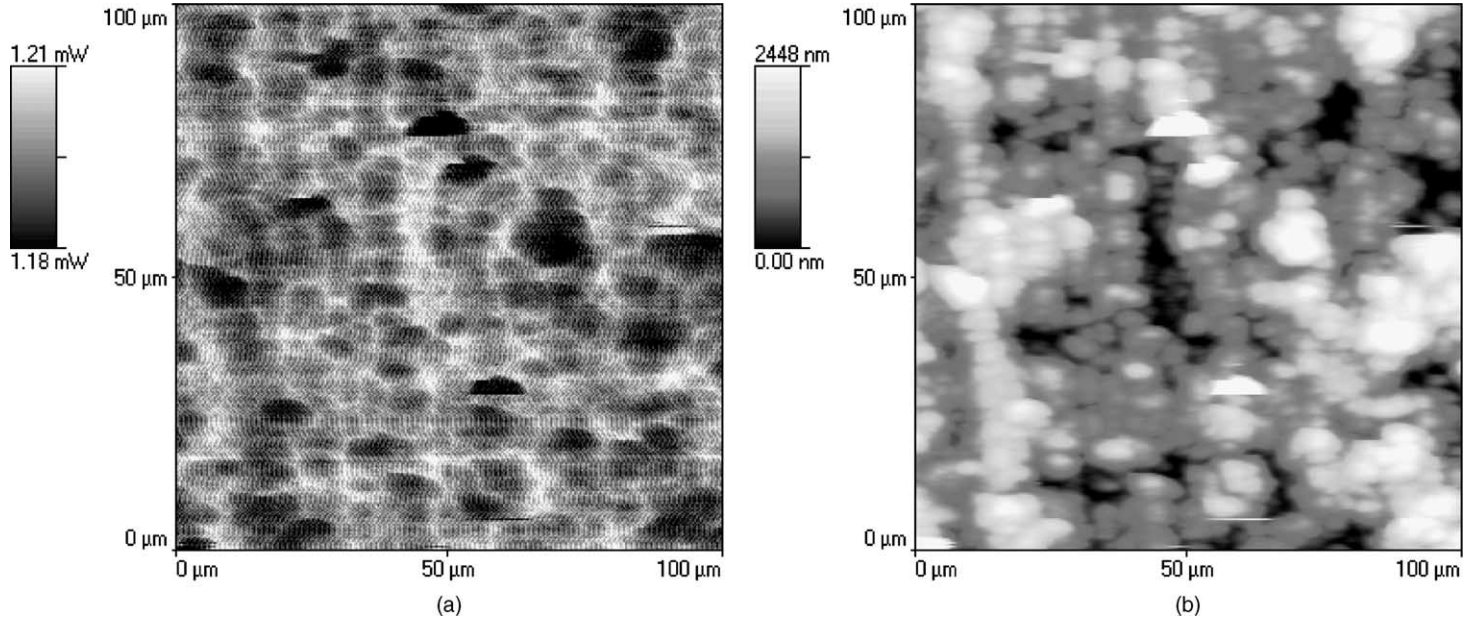

Fig. 1. (a) Thermal conductivity and (b) topography images at 55 °C and 2 kHz, for the normal area of the microtome sample 1.

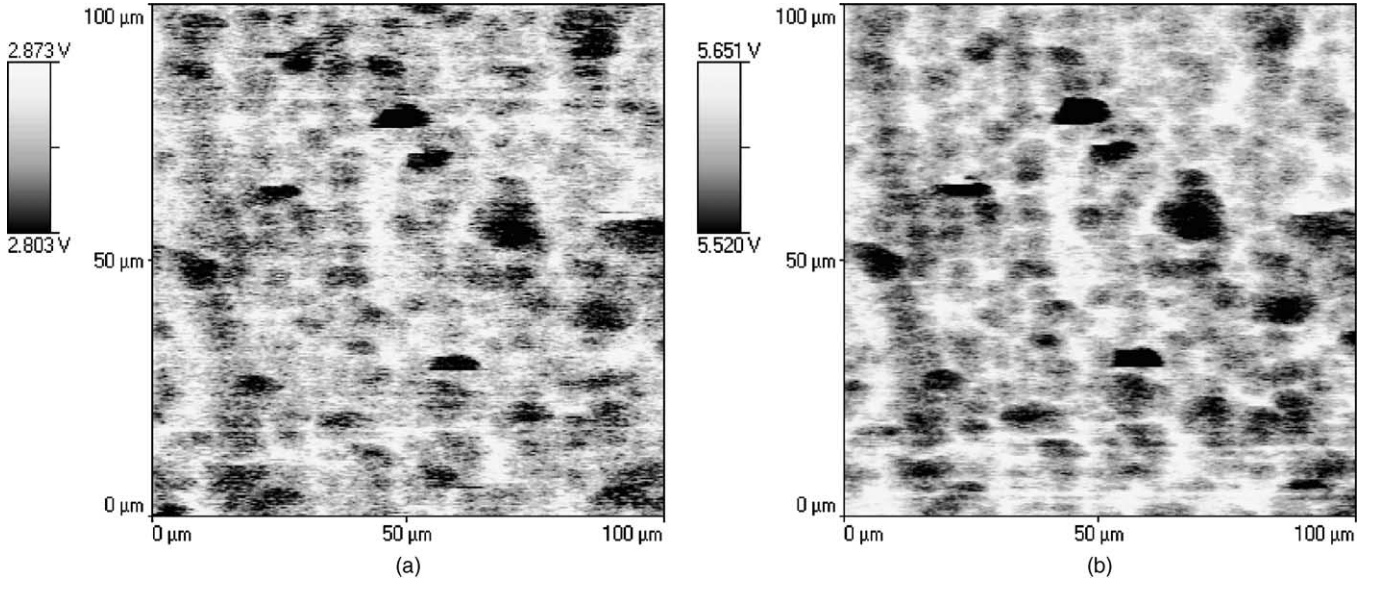

Fig. 2. Thermal diffusivity images for the normal area of microtome sample 1, at (a) 55 °C, 2 kHz and (b) 80 °C, 2 kHz.

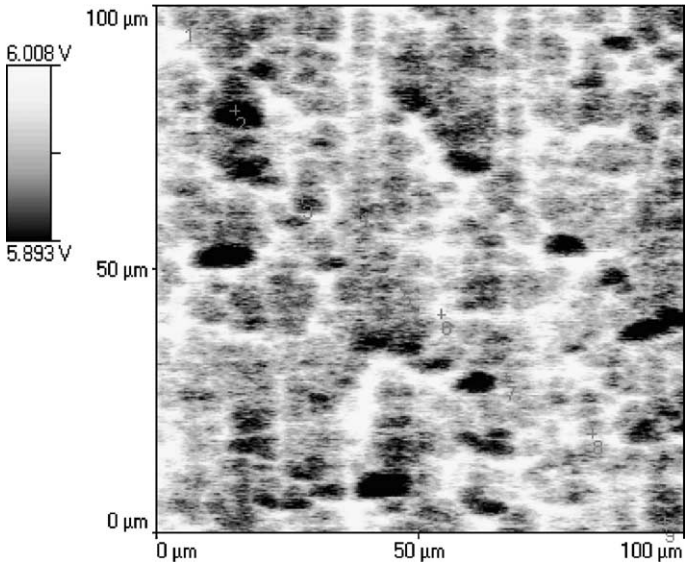

Fig. 3. Thermal diffusivity image for the dull area of microtome sample 3, at 80 °C and 2 kHz.

packing pressures result in alignment of the polyacrylate rubber particles and hence promote their coalescence [19]. Similar observations are also noted for sample 3, as shown in Fig. 3, which represents the thermal diffusivity scan (at 80 °C and 2 kHz) of the sample.

These images suggest that variations in the level of gloss, whether the surface is dull or glossy, is produced by variations in the number, type and size of rubber domains and their agglomerates. This may be a surface or near-surface phenomena caused by the packing conditions brought about by the injection of a molten material into a cold mold. The molten material is exposed to high shearing within the screw and nozzle, as well as in the mold where it is packed under high pressure. These conditions obviously have a significant effect on the rubber particle size and distribution, which will in turn have an effect on the surface finish of the product. Future work, directed at the surface will provide data on this hypothesis and is currently under way.

3.3. Effect of different processing conditions on surface roughness and morphology

The effect of different injection molding parameters on the surface finish and morphology was examined using plaque samples. Scans were performed at various temperatures and frequencies (55 and 80 °C, both at 2 and 64 kHz). Scanning at higher temperatures showed better resolution scans. Scans at 64 kHz were performed at the outer most layer of the sample plaque, whereas at 2 kHz, scans were achieved on the sub-surface (∼5 µm in depth). All scans were taken near the gate.

3.3.1. Ideal injection molding, plaque samples, normal area

The normal area of sample 1 shows wave-like features that are evenly spaced (Fig. 4a and b). Increasing the modulating frequency from 2 to 64 kHz results in the wave-like feature being seen with a larger area (Fig. 4b). This feature appears to represent the various phases of the polymer, not the flow direction. Similarly, sample 2 showed the same wave-like feature (Fig. 5). Sample 3, differed only in the breadth of the various phases, as compared to samples 1 and 2 and this is attributed to the different processing conditions.

3.3.2. Ideal injection molding, plaque samples, dull area

Sample 1 (at both frequencies) shows the lower conductivity particles aligned in cylindrical patterns from top to bottom, with the higher conductivity phase

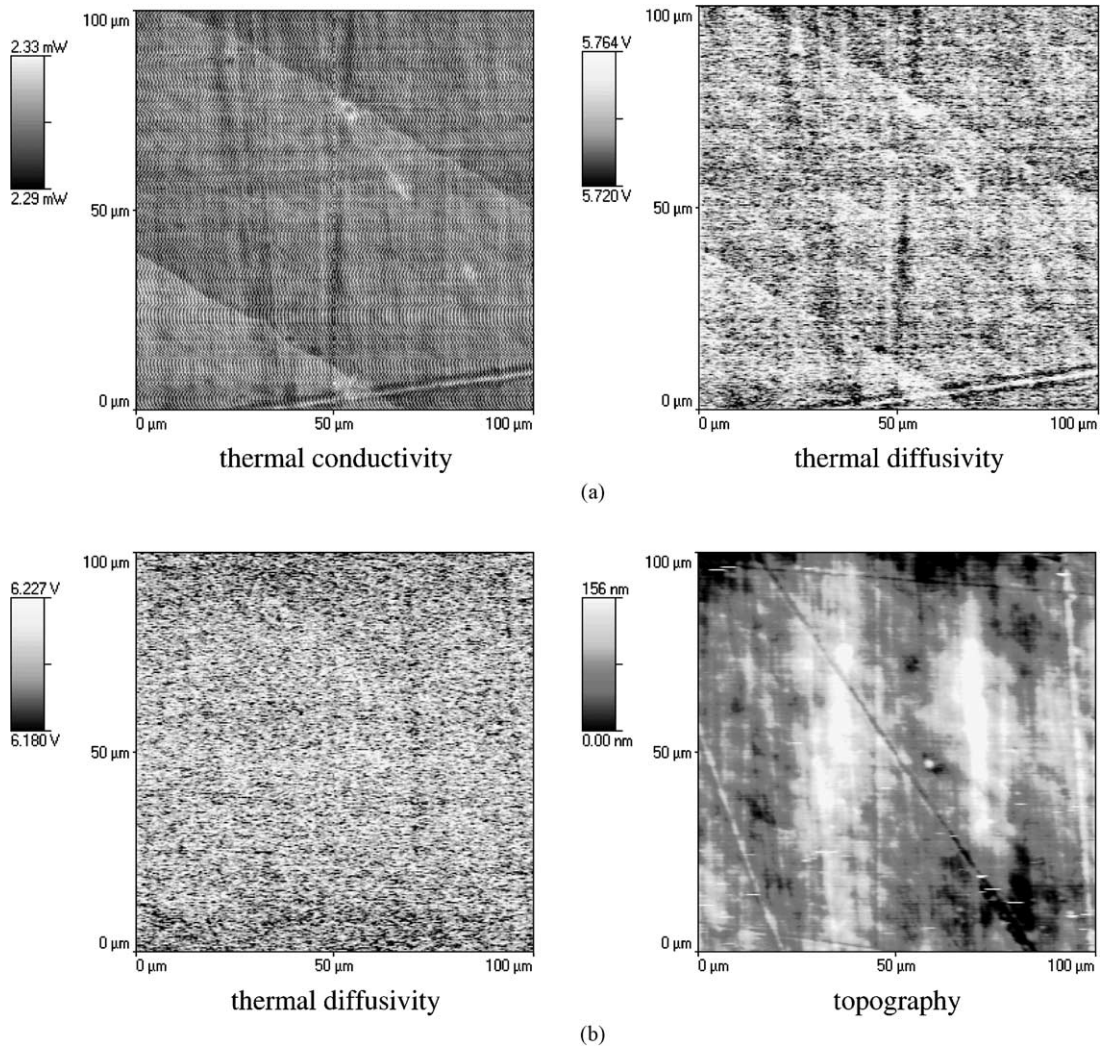

Fig. 4. Normal area plaque 1: (a) thermal conductivity and thermal diffusivity images at 80 °C and 2 kHz and (b) thermal diffusivity and topography images at 80 °C and 64 kHz.

in the background. These cylindrical patterns (or flow marks) are perpendicular to the flow and cannot be seen by the naked eye. These flow marks are said to form when the molten polymer near the mold wall at the advancing front is cooled to the no flow temperature of the resin, before it contacts the mold wall [8]. On thermal images, wave-like marks are observed at all frequencies and temperatures. These can be the boundaries of the different phases, which form wavy features due to wall slippage of the melt, or they can be an indication of the flow front, which flows from right to left. Cylindrical patterns are also observed for the dull area of sample 2 (Fig. 6). Fig. 6 shows the thermal conductivity images for the dull area of plaque 2 at 80 °C at both modulating frequencies (2 and 64 kHz). Cylindrical patterns are tightly packed when compared to sample 1 and this is due to the high pack pressure used in sample processing. There is also an even distribution of phases in different regions. The dull area of sample 3, processed at

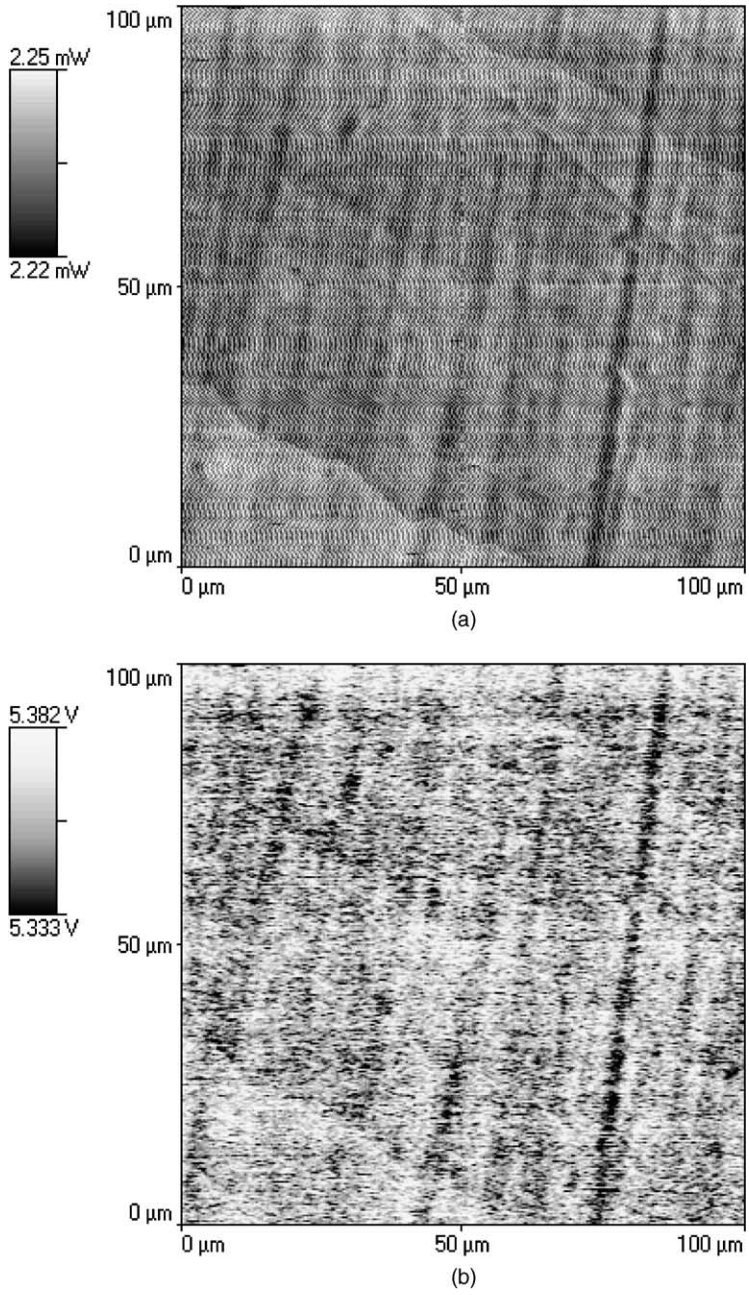

Fig. 5. (a) Thermal conductivity and (b) thermal diffusivity images at 80 °C and 2 kHz for normal area, plaque 2.

high material temperature, does not show the presence of any cylindrical features (as per samples 1 and 2) because of better flow properties as a result of the higher material temperature. Clear phase boundaries are seen, though these do vary slightly with an increase in modulated frequency. In addition, scans were performed for all samples at an angle of 90°, to ensure that the cylindrical features appeared in the

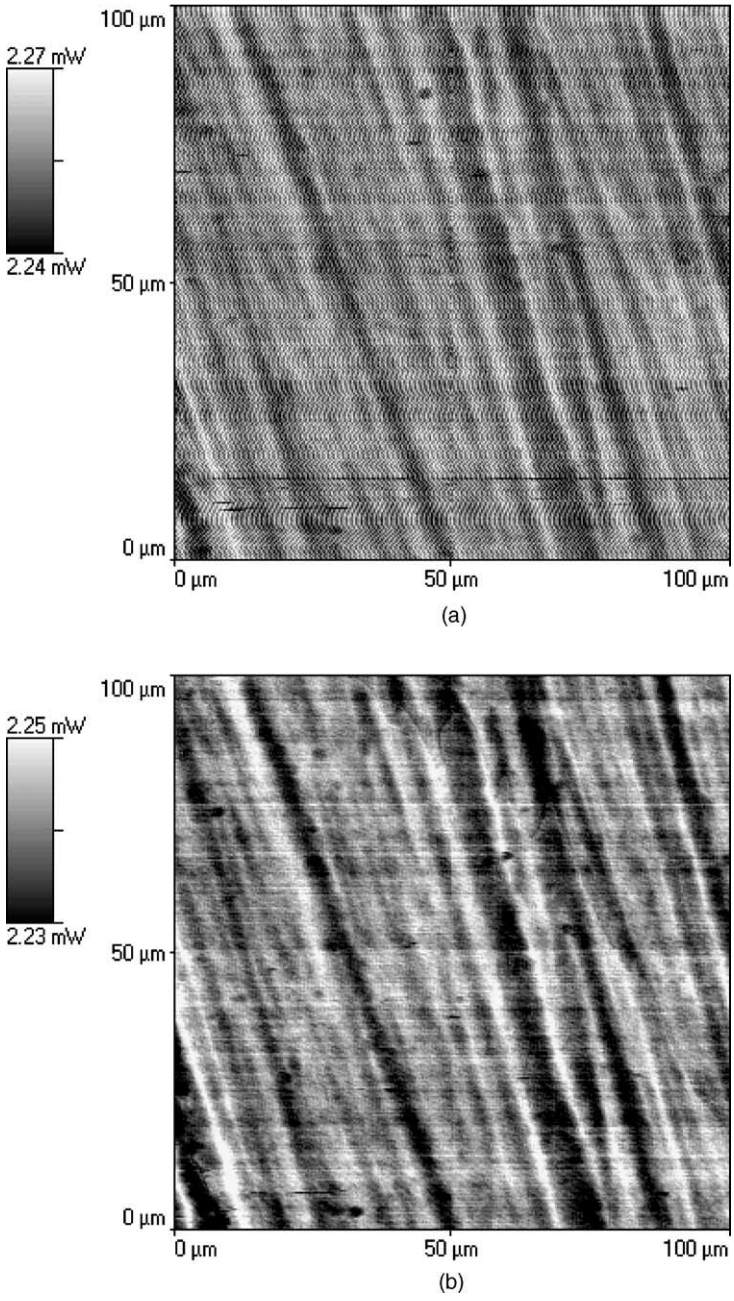

Fig. 6. Thermal conductivity images for the dull area of plaque 2, scanned at 80 °C at (a) 2 and (b) 64 kHz.

opposite direction, indicating that they are not due to artefacts.

The cylindrical features are then evident only on the dull area of samples 1 and 2. This may be attributed to differences observed between the normal and dull area, based on the degree of surface roughness and hence preferential phase segregation. The dull area, in general, appears rough whereas the normal area is smooth. The cylindrical shapes observed are an indication of the surface roughness.

3.4. Local thermal analysis (LTA)

In order to examine the effect of processing conditions on bulk and surface morphology, LTA (DC mode) was performed on up to nine various locations (low/high thermal conductivity areas) for both microtomed and plaque surfaces. Each LTA location is marked on the respective thermal image, as shown

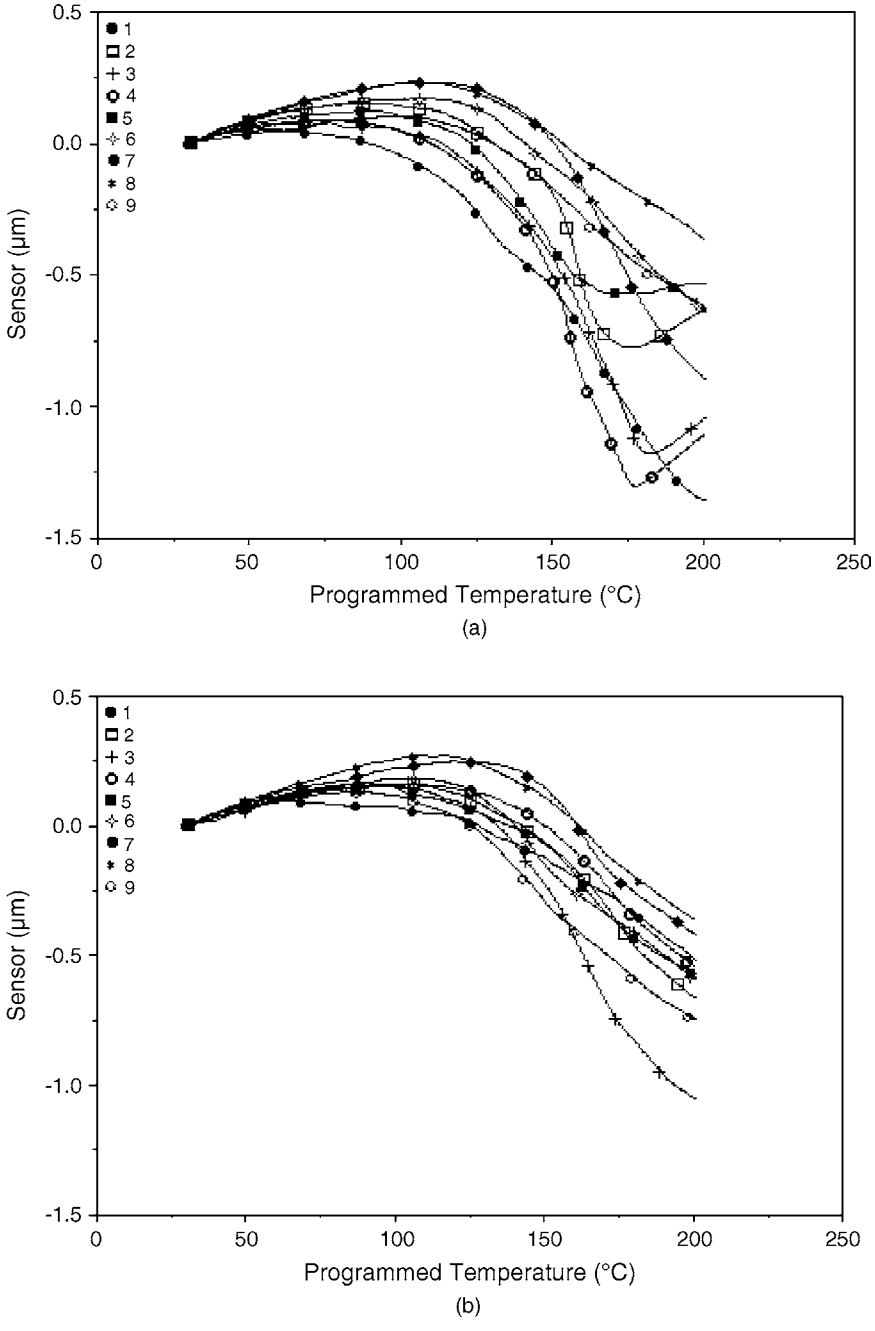

Fig. 7. LTA traces of microtomed samples (a) 1, (b) 2 and (c) 3 (dull areas).

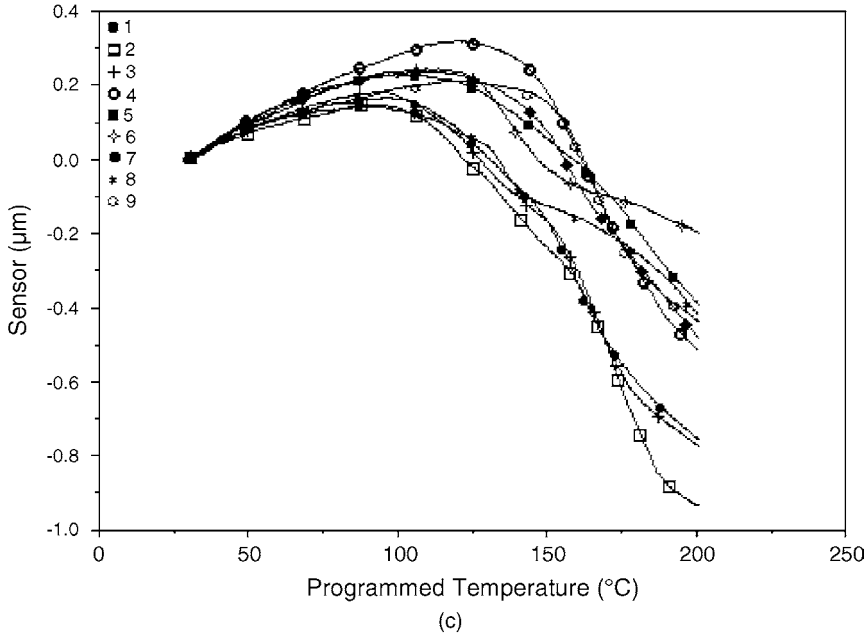

Fig. 7. (*Continued*).

in Fig. 3. All LTA traces are plotted with the sensor signal against programmed temperature. The sensor signal relates to the deflection of the probe in the z-plane as the tip is heated on the surface of the sample [10].

3.4.1. Microtomed samples

For microtomed samples 1–3, softening traces at various locations can be seen in Fig. 7a–c and the corresponding glass transition temperatures (T_g) are listed in Table 2. It is seen from Fig. 7a that, low T_g

Table 2
LTA for normal and dull areas of the microtomed samples

Sample (location)	T_g (°C) at various locations								
	1	2	3	4	5	6	7	8	9
1 (normal)	114.0	115.9	123.7	111.7	122.4	121.8	126.0	107.8	115.7
	127.5			140.3	145.7	140.8		137.8	
2 (normal)	115.4	120.2	131.9	116.0	95.99	142.6	125.3	131.1	143.2
	139.0	143.3	142.0	143.7	107.8		138.1		
					134.8				
3 (normal)	108.8	102.1	124.2	115.7	124.0	111.5	110.2	122.9	108.7
	138.6	123.6					128.0	143.6	126.7
									142.0
1 (dull)	100.9	99.29	97.40	101.6	99.27	120.4	121.8	117.7	122.2
	136.4		113.9	145.9	125.8	139.5		145.2	
2 (dull)	96.1	112.7	114.2	127.3	101.6	120.9	138.0	126.2	100.4
	121.5	143.1	138.2		125.0	139.0		143.7	125.1
	136.0								
3 (dull)	104.9	102.5	102.0	137.1	110.7	122.4	122.6	109.0	140.0
	115.9	123.8			123.1		141.0	125.0	
	137.9				142.3				

(T_g = 100–125 °C) are due to styrene acrylonitrile (SAN) grafted rubber domains, while the high T_g values (136–145 °C) are due to PC phase and the intermediate T_g is due to mixed phases or interphases (Table 2). Rubber particles are likely to be found in the low conductivity region; however, as no cooling facility is attached to our current μTA™, low T_g values could not be detected in this region. The rubber particles are

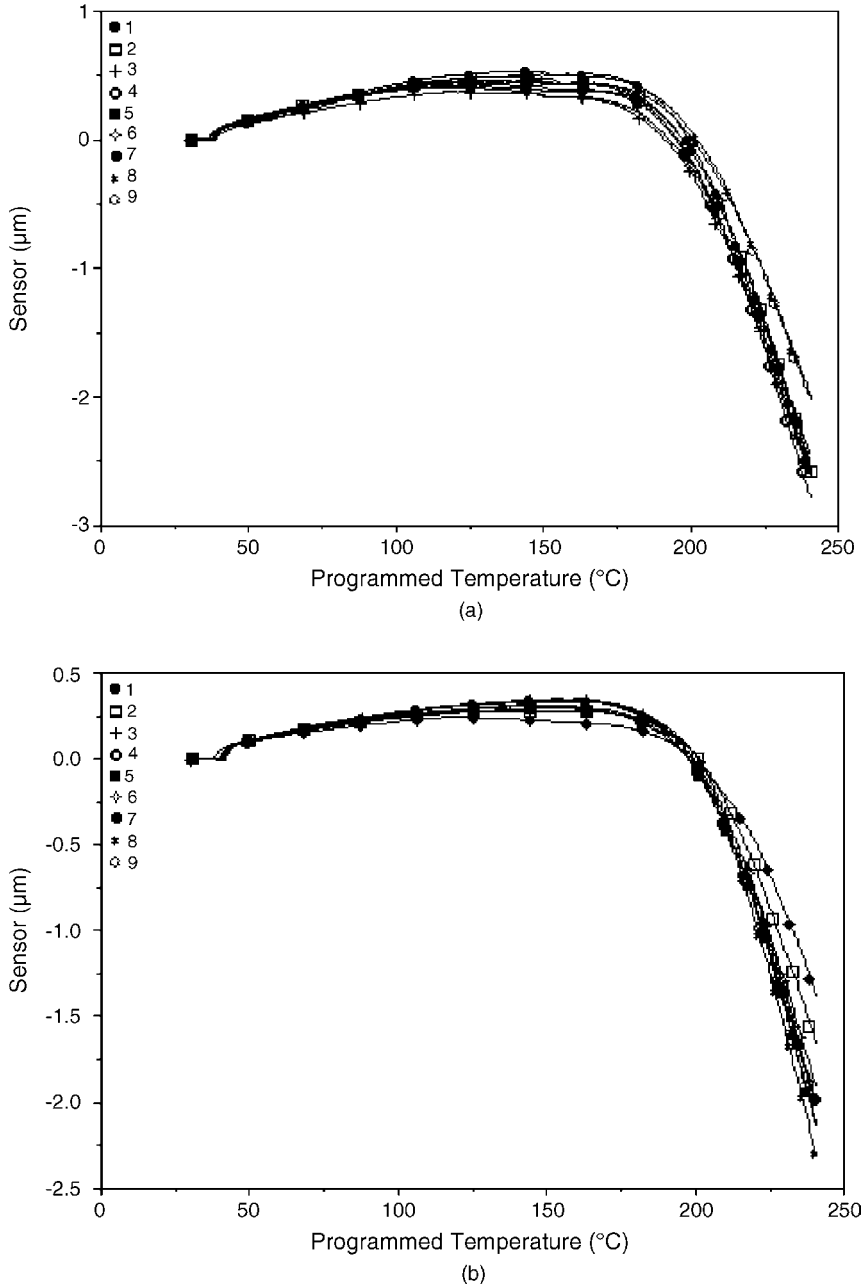

Fig. 8. LTA traces of plaque (a) sample 1 and (b) sample 3 (dull areas).

Table 3
LTA for normal and dull areas of plaque samples

Sample (location)	T_g (°C) at various locations								
	1	2	3	4	5	6	7	8	9
1 (normal)	96.4 126.4	137.4	172.6	146.3	155.1	168.6	159.4	161.6	156.0
2 (normal)	172.7	172.8	173.9	171.4	151.0	172.1	170.1	170.4	166.0
3 (normal)	160.9	165.5	171.3	173.8	181.2	174.0	174.8	165.6	173.6
1 (dull)	147.6	149.9	143.2	148.7	146.2	140.2	149.4	168.5	144.0
2 (dull)	156.0	118.0 159.7	172.5	110.8 143.1	171.7	171.9	166.3	117.0 148.6	169.7
3 (dull)	175.7	172.0	173.1	173.5	164.8	157.4	132.0 155.8	168.1	173.3

embedded in a SAN shell. This structure enhances physical properties such as toughening from the rubber component, rigidity from the styrene component and hardness from the acrylonitrile component [15]. Differences in gloss between the dull edge and normal area for all samples are due to the aggregation of rubber particles at the surface.

Increasing the applied pack pressure (sample 2) results in different softening traces as compared to the ideal set up. Fig. 7b (dull edge) shows the softening traces at various locations of the microtomed sample 2. From this scan, it is clear that in some locations two transitions exist, with the high conductivity region showing T_g of SAN (100–125 °C) and PC (136–143 °C) (Table 2). As the amount of PC in the total formulation is small, there is therefore, only a small descent in slope observed. From the T_g of the low conductivity regions of sample 2 for both normal and dull areas, PC shows a T_g of 136–143 °C (Table 2). Also, the T_g value of low conductivity region indicates the presence of SAN and rubber particles, with the medium zones consisting mainly of the SAN matrix for both dull and glossy areas.

Fig. 7c represents the softening curves of microtomed sample 3. Higher orientation occurring in the medium conductivity region of the dull edge is observed, with PC and SAN glass transitions detected. Areas of high and low thermal conductivity reveal that they consist primarily of SAN (100–123 °C). For the normal area, both the high and medium regions consist of purely the SAN matrix and the low region consists of both PC (137–142 °C) and SAN (Table 2).

Sample 3 visually showed more surface defects as compared to samples 1 and 2. The orientation of particles, as seen from the LTA data, shows that the detection of PC influences the appearance of the samples surface finish. In certain regions for the dull and normal areas, there is more than one T_g. This represents that at a particular area, more than one component is present in a multiphase arrangement.

3.4.2. Plaque samples

The softening traces for plaque samples 1 and 3 (dull area) can be seen in Fig. 8a and b. All LTA softening traces for the plaque samples reveal clear and reproducible results, showing the presence of a dominant PC phase at the surface. This is a result of a solidified skin layer forming at the surface of the mold. As the molten plastic is injected into a cold mold, a very thin layer of polymer will instantly freeze and form a solidified layer or 'skin' at the surface of the mold. It is theorised that variations in the homogeneity of this skin layer is responsible for the formation of defects, such as flow and stress marks on the surface of injection molded polymeric blends [20].

Data from Table 3 shows that PC is the dominant material found in the normal areas for all plaques at various injection molding processing conditions. The dull areas however, were found to be rich in both PC and ASA. This phenomenon is due to each material's flow and viscosity characteristics, which promotes preferential phase segregation. In the blend, PC is the lower molecular weight component and thus flows well and consequently forms the skin layer for those

parts produced with a glossy finish. ASA on the other hand, has a high viscosity and flows poorly and sits as a droplet. In the case of a high viscosity polymer melt, the flow front travels towards the mold thickness direction, resulting in high shear stress on the PC and ASA. As PC has higher shear sensitivity than ASA, the flow front may contain both a PC and ASA phase. This melt front will therefore flow to the mold wall, form the skin and generate a dull area on the plaque surface [20]. Another cause for preferential phase segregation of PC phase to the mold's surface can be due to the high surface energy of the mold plus PCs high surface energy (42 mN/m) as compared to SAN (38 mN/m) [21].

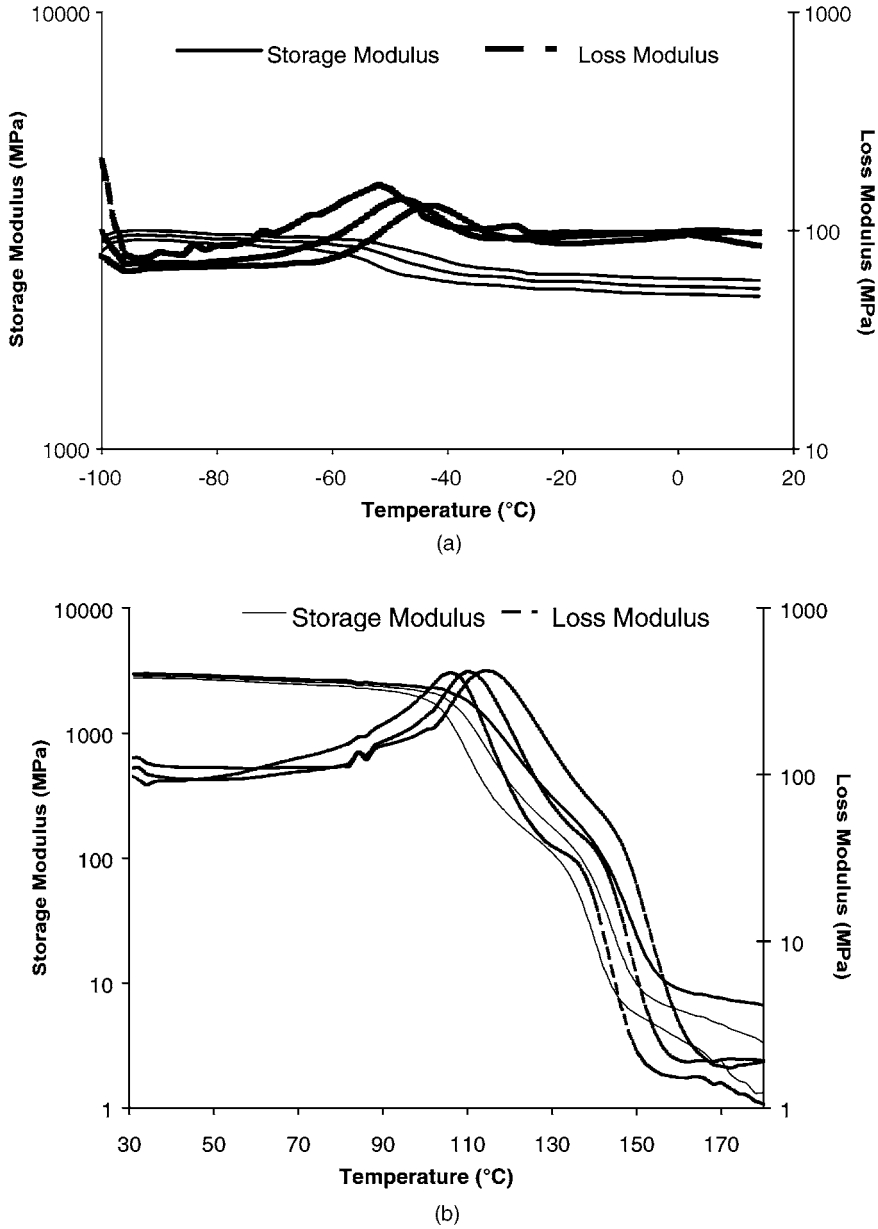

Fig. 9. (a) Low and (b) high temperature plots at varying frequencies from left to right; 0.1, 1 and 10 Hz for plaque 1.

It is interesting to note that T_g values obtained for the plaque samples are higher than the reference value. This is thought to be the result of varying processing and experimental conditions that occurred during molding. Additionally, the LTA traces of microtomed samples show more of a distribution because analysis occurs within the core of the samples. This is believed to be due to two reasons:

1. Depending on the injection molding conditions, various phases may co-exist on the surface or subsurface of the molded part. Therefore, T_gs will be governed by the weight fraction of each phase/component present in that particular location.
2. The presence of rubber particles in the blend, both bound and unbound, will affect the mobility of matrix chain segments. Those polymeric chains, in close proximity to a particle, will exhibit a higher T_g value than those further away.

Future work will look at quantifying these phenomena through other morphological studies. However, this has not been investigated in this work.

3.5. Phase behaviour and morphology by DMA

DMA was carried out in two stages (from subambient to room temperature and from room temperature to high temperature) to investigate the morphology. Fig. 9a and b show representative plots of the effect of temperature on storage modulus and loss modulus at varying frequencies for plaque 1. The transition from glassy state, through the rubbery state, to the region of viscous flow can clearly be identified. Three distinct steps in storage modulus, corresponding to peaks in the loss modulus curves identify the three T_gs (Table 4) of the PC/ASA blend, indicating an immiscible rubber-modified thermoplastic. These T_gs represent the acrylate rubber, (SAN) and (PC) phases. From the broad transition observed between temperatures 90–120 °C at 0.1 Hz (Fig. 9b), it is evident that two components are present. PMMA has been shown as a minor component from the T_g values from μTA and it appears around 85–90 °C. From Fig. 9b, broadness of the transition indicates that PMMA remains compatible in the SAN phase at this proportion. All plaques show consistent values for their glass transitions, which as expected, increase with increasing frequency. The trend in T_g values obtained, correlates with the morphology and T_g values obtained by LTA, for the PC and SAN phases.

Table 4
Glass transition temperatures determined by DMA

Plaque	Phase	T_g (°C) at varying frequencies (Hz)		
		0.1	1	10
1	Acrylate	−52.1	−48.2	−43.2
	SAN	106.0	110.1	114.2
	PC	136.0	139.3	149.3
3	Acrylate	−52.2	−48.5	−44.1
	SAN	104.9	109.2	114.2
	PC	136.0	139.3	143.2

4. Conclusions

In this study, injection molded samples, which commonly produce surface defects inherent to the processing technique, have been characterised by μTA™ and DMA. It is clearly evident from these analyses that multiphase morphology is present and that each phase can now be individually characterised via a single analytical technique.

By varying the injection molding processing conditions, it has been found that such variations influence the average particle size. μTA™ also showed distinct and clearly defined particle morphology in the normal (glossy) area, however, the gloss variation observed for all samples, is a direct result of particle agglomeration.

Multiphase morphology is evident from the examination of the microtomed samples, where several glass transition temperatures were observed, confirming the co-existence of localised phases. Also from depth profiling (plaque samples) and its corresponding LTA, it is seen that PC and ASA are rich at the outermost surface in the dull area, indicating multiphase segregation arising from changes in processing conditions. As a result, in the vicinity of a rubber particle, mobility is restricted and a higher T_g of a phase is observed. Thus combination of a new analytical technique such as μTA™ with the more conventional DMA allows for an accurate determination of morphology, helping understand our knowledge of surface defects in injection molded polymers.

Acknowledgements

The authors are thankful to TA Instruments for helpful discussions and Australian Research Council (ARC) for support of this work through the collaborative grant scheme.

References

[1] P. Kennedy, Flow Analysis of Injection Molds, Hanser, 1995.
[2] G.A. Campbell, H. Devanathan, S. Settlemire, P. Sweeney, K. Klewicki, T. Kenny, J.D. Smael, A.L. Fricke, in: Proceedings of ANTEC, 1989, pp. 312–315.
[3] T.P. Skourlis, C. Mohapatra, C.S. Manochechri, Adv. Polym. Technol. 16 (2) (1997) 117–128.
[4] W.C. Bushko, V.K. Stokes, Polym. Eng. Sci. 35 (4) (1995) 365–383.
[5] M.C.O. Chang, in: Proceedings of ANTEC, 1994, pp. 312–315.
[6] J.D. Ferry, Viscoelastic Properties of Polymers, 3rd Edition, Wiley, New York, 1980.
[7] O.B.G. Assis, R. Bernardes-Filho, J.D.C. Pessoa, Electron Microscopy, 1998, pp. 703–704.
[8] M.M. Yoshii, H. Kuramoto, T. Kawana, Polym. Eng. Sci. 36 (6) (1996) 819–826.
[9] Technical Applications Note—TA 243, μTA 2990 Micro-Thermal Analyzer: Characterizing the Nano-World, TA Instruments (A Subsidiary of Waters Corp.), Newcastle, DE, USA.
[10] P.G. Royall, D.Q.M. Craig, D.M. Price, M. Reading, T.J. Lever, Int. J. Pharmaceutics 192 (1) (1999) 97–103.
[11] A. Hammiche, M. Reading, H.M. Pollock, M. Song, D.J. Houston, Rev. Sci. Instrum. 67 (12) (1996) 4268–4274.
[12] D.M. Price, M. Reading, A. Hammiche, H.M. Pollock, Int. J. Pharmaceutics 192 (1) (1999) 85–96.
[13] D.M. Price, M. Reading, Adv. Polym. Technol. 18 (1) (1999) 69–73.
[14] US Patent Numbers 5,248,199, 5,441,343, 5,469,734 (1998).
[15] S. Clarke, M.G. Markovic, N.R. Choudhury, J. Matisons, T. Levor, Chem. Aust. 66 (4) 1999.
[16] I. Moon, P. Androsch, W. Chen, B. Wunderlich, J. Therm. Anal. Calorimetry 59 (2000) 187–203.
[17] S.A. Edwards, M. Provatas, N.R. Choudhury, J.G. Matisons, Int. J. Mater. Product Technol., in press.
[18] C.B. Bucknall, Rubber Modified plastics, Generic Polymer Systems and Applications, Pergammon Press, Oxford, 1989 (Chapter 2).
[19] M. Provatas, S.A. Edwards, N. Roy Choudhury, J.G. Matisons, in: Proceedings of 28th NATAS, Orlando, Florida, 4–6 October 2000, pp. 39–44.
[20] H. Hamada, H. Tsunasawa, J. Appl. Polym. Sci. 60 (1996) 353–362.
[21] C.P. Radar, S. Abdou-Sabet, Thermoplastic Elastomers from Rubber–Plastic Blends, Ellis Horwood, UK, 1990 (Chapter 6).